RF PERFORMANCE OF INGOT NIOBIUM CAVITIES OF MEDIUM-LOW PURITY*

G. Ciovati#, P. Dhakal, P. Kneisel, J. Spradlin, G. Myneni, JLab, Newport News, VA 23606, USA

Abstract

Superconducting radio-frequency cavities made of ingot niobium with residual resistivity ratio (RRR) greater than 250 have proven to have similar or better performance than fine-grain Nb cavities of the same purity, after standard processing. The high purity requirement contributes to the high cost of the material. As superconducting accelerators operating in continuous-wave typically require cavities to operate at moderate accelerating gradients, using lower purity material could be advantageous not only to reduce cost but also to achieve higher Q_0-values, because of the well-known dependence of the BCS-surface resistance on mean free path. In this contribution we present the results from cryogenic RF tests of 1.3-1.5 GHz single-cell cavities made of ingot Nb of medium (RRR=100-150) and low (RRR=60) purity from different suppliers. Cavities made of medium-purity ingots routinely achieved peak surface magnetic field values greater than 70 mT with Q_0-values above 1.5×10^{10} at 2 K. The performances of cavities made of low-purity ingots were affected by significant pitting of the surface after chemical etching.

INTRODUCTION

The performance of superconducting radio-frequency (RF) cavities is described by a plot of the quality factor, Q_0, as a function of the accelerating gradient, E_{acc}, or as a function of the peak surface magnetic or electric fields, B_p and E_p, respectively, measured at or below 4 K. R&D efforts throughout the world over the last decade demonstrated that the performance of SRF cavities built from large-grain, ingot material is comparable to that achieved using standard fine-grain, bulk Nb [1]. A relatively small production series of 1.3 GHz, 9-cell cavities made of high-purity (RRR~300) ingot Nb material showed that high gradients, greater than ~40 MV/m, could be achieved reproducibly and that higher Q_0-values than those of cavities of the same shape made of fine-grain, high-purity Nb, were achieved at 2 K [2]. The push for higher purity material stemmed from the need to increase the thermal conductivity of the Nb in order to "thermally stabilize" defects in the material which can cause quenches at reduced gradients [3]. The production of high-purity, fine-grain Nb sheets requires many elaborate steps during which foreign metallic impurities can be embedded in the material and therefore requiring time-consuming quality control of the sheets [4]. The cost of high-purity, fine-grain Nb sheets is significant and exceeds ~600 $/kg. The production of ingot Nb discs is comparatively much simpler and therefore lower cost is to be expected. Whereas SRF cavities for high-energy particle colliders need to operate at gradients corresponding to B_p-values greater than ~100 mT, SRF cavities for continuous wave (CW) accelerators require operation at 70-80 mT but with high (> $\sim1\times10^{10}$ at 2 K) quality factor. The purity of the Nb material is a parameter which affects cost, quench field and surface resistance. In this contribution, we present the results of RF tests of 1.3-1.5 GHz single-cell cavities made of ingot Nb material with RRR in the range 60-150 to evaluate whether an "optimum" RRR from the cost-performance point of view can be found for CW accelerator cavities. The treatment processes included buffered chemical polishing (BCP), electropolishing (EP), centrifugal barrel polishing (CBP), annealing in vacuum (HT), low-temperature baking (LTB) and HF rinse (HF). The mechanical properties of medium-purity ingot Nb cavities have been recently evaluated and the yield pressure was found to be higher than that of high-purity, fine-grain Nb cavities [5].

CAVITY MATERIAL

Table 1 summarizes the cavities, material supplier and RRR used for this study. 1.3 GHz cavities are of the TESLA center-cell shape [6], whereas the 1.5 GHz cavities are of the original CEBAF shape [7]. The RRR was calculated from the resistance of $1 \times 1 \times 30$ mm^3 samples, measured with the standard four-probe method with an estimated error of 10%. The RRR calculated from the thermal conductivity at 4 K measured on another set of samples from ingots F, G, H was 126, 144 and 93, respectively.

Table 1: Cavity label, frequency, material supplier and average RRR values from 4-probe method and thermal conductivity at 4 K.

Cavity Label	Freq. (MHz)	Nb supplier /Ingot label	RRR
LG-RG	1.5	Tokyo Denkai	140 ± 10
F1F2	1.3	CBMM/F	118 ± 11
F5F6	1.5	CBMM/F	118 ± 11
G1G2	1.5	CBMM/G	125 ± 20
H1H2	1.5	CBMM/H	100 ± 10
H3H4	1.5	CBMM/H	100 ± 10
TC1N1	1.3	OTIC	60 ± 6
OCC1N2	1.5	OTIC	60 ± 6

* This manuscript has been authored by Jefferson Science Associates, LLC under U.S. DOE Contract No. DE-AC05-06OR23177. The U.S. Government retains a non-exclusive, paid-up, irrevocable, world-wide license to publish or reproduce this manuscript for U.S. Government purposes.
#gciovati@jlab.org

ISBN 978-3-95450-178-6

CAVITY PREPARATION AND TEST RESULTS

LG-RG

Figure 1 shows the evolution of the quench field and of the quality factor at 2.0 K at low field (18 mT) and at 70 mT, for different treatments after fabrication. The "1400C/3h" and "2N10+7µm EP" correspond to Ti [8] and N doping [9], respectively, and resulted in a drastic reduction of the quench field. No field emission was detected in any of the tests. The reduction of Q_0 as the field increased from 18 mT to 70 mT is <10% on average. Table 2 shows the average residual resistance, R_{res}, and BCS surface resistance at 4.3 K, R_{BCS}(4.3 K), obtained from the measurement of R_s versus He bath temperature, T, at 5 mT:

$$R_s(T) = \frac{G}{Q_0(T)} = R_{res} + R_{BCS}(T, \Delta, \ell). \qquad (1)$$

G is the cavity geometry factor, Δ is the energy gap and ℓ is the mean free path. R_{res}, Δ and ℓ are fit parameters and R_{BCS} is calculated using Halbritter's program [10] to solve Mattis-Bardeen integrals, assuming the critical temperature to be 9.25 K, the coherence length to be 39 nm and the London penetration depth to be 32 nm.

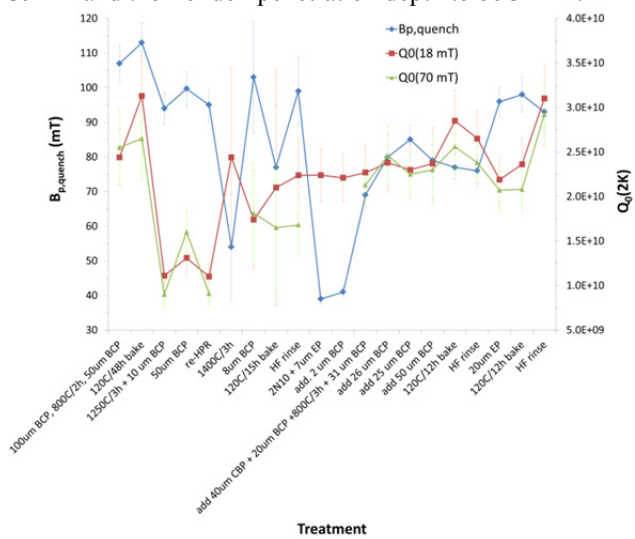

Figure 1: Evolution of the quench field and Q_0(2 K) at 18 mT and 70 mT for the 1.5 GHz cavity LG-RG after multiple treatments, listed chronologically on the abscissa.

The average values of Δ/k_BT_c after BCP/EP and LTB are 1.80 ± 0.01 and 1.910 ± 0.002, respectively. The average values of ℓ after BCP/EP and LTB are (89 ± 38) nm and (26 ± 44) nm, respectively. Δ/k_BT_c and ℓ after HF rinse, following LTB, did not change. The average quench field measured at 2 K after a final treatment of BCP is (84 ± 2) mT, whereas it was (96 ± 4) mT after EP.

Table 2: Average R_{res} obtained from a fit of R_s(T) with Eq. (1) and average R_{BCS}(4.3 K, 5 mT) and Q_0(2 K, 70 mT) measured after BCP/EP, LTB and HF rinse on 1.5 GHz cavity LG-RG.

Treatment	R_{res} (nΩ)	R_{BCS} (nΩ)	Q_0 (×10^{10})
BCP/EP	2.1 ± 0.1	698 ± 11	2.1 ± 0.1
LTB	4.8 ± 0.1	578 ± 11	2.3 ± 0.2
HF rinse	2.6 ± 0.1	593 ± 14	2.3 ± 0.2

F1F2 and F5F6

Figure 2 shows the evolution of the maximum field and Q_0(2 K) at low and medium field for different treatments applied to cavity F1F2 after fabrication. Field emission did not occur during any of the tests, however, strong multipacting inducing quenches, often occurred in the range 70-100 mT. Tests where multipacting limited the maximum field are shown by arrows in Fig. 2.

The cavity F5F6 was tested once after 100 µm removal by CBP, 50 µm removal by BCP, HT at 800 °C/2 h, 20 µm removal by BCP. The quench field of F5F6 was (85 ± 6) mT and the Q_0(2 K, 70 mT) was (1.7 ± 0.3)×10^{10}.

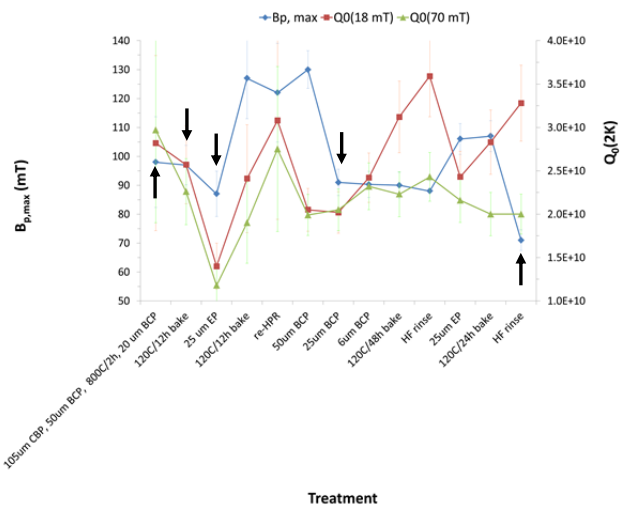

Figure 2: Evolution of the quench field and Q_0(2 K) at 18 mT and 70 mT for the 1.3 GHz cavity F1F2 after multiple treatments, listed chronologically on the abscissa. The arrows indicate tests with multipacting induced quenches.

The average R_{res} obtained from a fit of R_s(T) with Eq. (1) and the average R_{BCS}(4.3 K, 5 mT) and Q_0(2 K, 70 mT) measured after BCP/EP, LTB and HF rinse for cavity F1F2 are shown in Table 3. A strong medium-field Q-slope occurred after LTB in the last two etching+LTB cycles, causing the Q_0(70 mT) not to improve compared to the values after BCP/EP. HF rinsing did not affect the medium field Q-slope.

The average values of Δ/k_BT_c after BCP/EP and LTB are 1.84 ± 0.01 and 1.89 ± 0.01, respectively. The average values of ℓ after BCP/EP and LTB are (138 ± 10) nm and (36 ± 16) nm, respectively. Δ/k_BT_c and ℓ after HF rinse

did not change after LTB. The average maximum field achieved after BCP in cavities F1F2 and F5F6 is (96 ± 3) mT, the same as the average maximum field in cavity F1F2 after EP.

Table 3: Average R_{res} obtained from a fit of R_s(T) with Eq. (1) and average R_{BCS}(4.3 K, 5 mT) and Q_0(2 K, 70 mT) measured after BCP/EP, LTB and HF rinse on 1.3 GHz cavity F1F2.

Treatment	R_{res} (nΩ)	R_{BCS} (nΩ)	Q_0 (×10^{10})
BCP/EP	2.4 ± 0.1	653 ± 8	1.9 ± 0.1
LTB	3.8 ± 0.1	446 ± 9	2.1 ± 0.2
HF rinse	2.1 ± 0.1	449 ± 9	2.2 ± 0.2

G1G2

Figure 3 shows the evolution of the maximum field and Q_0(2 K) at low and medium field for different treatments applied to cavity G1G2 after fabrication. There was no field emission in any of the tests. However, multipacting at ~80 mT was sometimes observed and it could have induced quenches in the tests marked by arrows in Fig. 3. The treatments "1250C/3h", "1300C/3h" and "1400C/3h" resulted in doping of the Nb surface with Ti, resulting in the increase of Q_0(2 K) over a broad field range. The treatment "2N10, 7um EP" consists of doping the Nb surface with N by admitting ~20 mTorr N_2 gas at 800 °C for 2 min, after the cavity had been annealed in vacuum at 800 °C/3 h, followed by soaking at 800 °C/10 min in vacuum. Doping resulted in Q_0-values at 2 K higher than ~2.5×10^{10} but the quench field is reduced significantly.

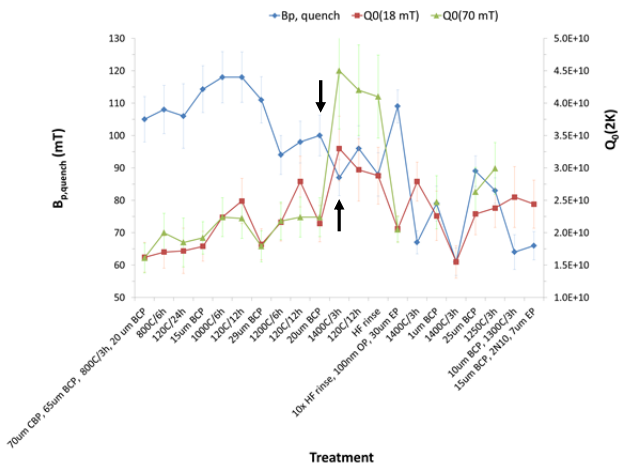

Figure 3: Evolution of the quench field and Q_0(2 K) at 18 mT and 70 mT for the 1.5 GHz cavity G1G2 after multiple treatments, listed chronologically on the abscissa. The arrows indicate tests for which quench could have been caused by multipacting.

The average R_{res} obtained from a fit of R_s(T) with Eq. (1) and the average R_{BCS}(4.3 K, 5 mT) and Q_0(2 K, 70 mT) measured after BCP/EP, annealing (without subsequent chemical etching) and LTB for cavity G1G2 are shown in Table 4. Data from tests after Ti or N doping are not considered. The values of R_{BCS} in Table 4 correlate with the values of ℓ from the R_s(T) fit. The average quench field achieved after BCP is (96 ± 2) mT.

Table 4: Average R_{res} obtained from a fit of R_s(T) with Eq. (1) and average R_{BCS}(4.3 K, 5 mT) and Q_0(2 K, 70 mT) measured after BCP/EP, annealing and LTB on 1.5 GHz cavity G1G2.

Treatment	R_{res} (nΩ)	R_{BCS} (nΩ)	Q_0 (×10^{10})
BCP/EP	2.2 ± 0.1	788 ± 11	2.0 ± 0.1
800-1200°C	2.1 ± 0.2	1020 ± 20	2.1 ± 0.2
LTB	2.3 ± 0.2	652 ± 15	2.1 ± 0.2

H1H2 and H3H4

Figure 4 shows the evolution of the maximum field and Q_0(2 K) at low and medium field for different treatments applied to cavities H1H2 and H3H4 after fabrication. There was no field emission in any of the tests, which were limited by quench.

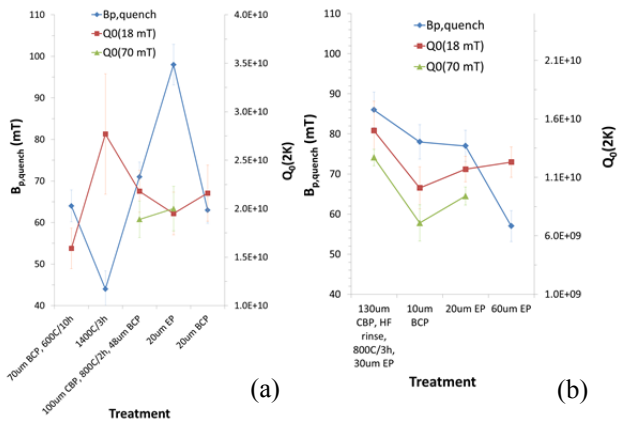

Figure 4: Evolution of the quench field and Q_0(2 K) at 18 mT and 70 mT for the 1.5 GHz cavities H1H2 (a) and H3H4 (b) after multiple treatments, listed chronologically on the abscissa.

The half-cell H1 was etched by BCP to remove ~70 µm from the inner surface prior to welding to half-cell H2 and pits were visible in an area of the inner surface after etching. Half-cell H2 was annealed at 800 °C/5 h prior to equator welding. After the cavity fabrication was completed, temperature mapping during the test after 70 µm BCP and 600 °C/10 h annealing, showed the quench to be in the pitted region. The following annealing at 1400 °C/3 h improved the Q_0-value but the cavity quenched at lower field at the same location. The quench location changed after 100 µm CBP, 800 °C/2 h HT and 48 µm BCP and the quench field increased up to ~100 mT after EP. No feature was visible at the new quench location.

ISBN 978-3-95450-178-6

The half-cells H3 and H4 were annealed at 1200 °C/3 h prior to equator welding. Temperature maps taken during tests showed that the quench location changed after additional chemistry. Optical inspection showed isolated pits visible at the quench spots, except after the last test, after 60 µm EP, where a cluster of pits was present. The Q_0-values of cavity H3H4 is nearly a factor of two lower than that of H1H2 due to higher R_{res}. Table 5 lists the average R_{res}, Δ/k_BT_c and ℓ obtained from a fit of $R_s(T)$ with Eq. (1), and the average R_{BCS}(4.3 K, 5 mT) and Q_0(2 K, 70 mT) measured after BCP/EP for cavities H1H2 and H3H4.

The quench field value averaged over the tests and cavities is (72 ± 8) mT after BCP and (86 ± 15) mT after EP.

Table 5: Average R_{res}, Δ/k_BT_c and ℓ obtained from a fit of $R_s(T)$ with Eq. (1) and average R_{BCS}(4.3 K, 5 mT) and Q_0(2 K, 70 mT) measured after BCP/EP on 1.5 GHz cavities H1H2 and H3H4.

	H1H2	H3H4
R_{BCS}(4.3 K) (nΩ)	770 ± 16	789 ± 13
R_{res} (nΩ)	1.1 ± 0.2	8.7 ± 0.2
Δ/k_BT_c	1.82 ± 0.01	1.77 ± 0.01
ℓ (nm)	97 ± 19	70 ± 22
Q_0(2 K, 70 mT) ($\times 10^{10}$)	1.9 ± 0.1	0.8 ± 0.1

TC1N1 and OCC1N2

The four ingot Nb discs from OTIC, Ningxia, were eddy-current scanned at DESY and no defects were found. The discs were etched by BCP to remove ~20 µm from each side, followed by annealing at 800 °C/3 h. After standard fabrication, the cavities were treated as follows: 60-80 µm removal from the inner surface by BCP, annealing at 800 °C/3 h, 15-50 µm BCP. The inner surface of both cavities had very dense, uniform pitting. The RF tests at 2.0 K showed a sharp drop of Q_0, decreasing from ~2×10^{10} at ~3 mT to ~1.5×10^{9} at 18 mT for TC1N1 and from ~2×10^{10} at ~8 mT to ~5×10^{9} at 28 mT for OCC1N2, with no field emission. CBP followed by EP was done to both cavities to eliminate the pits. The performance of both cavities greatly improved after CBP, HT, EP, but only in one case a quench field of 70 mT was reached after additional EP. Figure 5 shows the evolution of the quench field and Q_0(2 K) for both cavities whereas the average R_{res}, Δ/k_BT_c and ℓ obtained from a fit of $R_s(T)$ with Eq. (1), and the average R_{BCS}(4.3 K, 5 mT) are listed in Table 6. The central portion of one of the discs used to fabricate the cavities was etched by BCP to remove ~100 µm and the surface showed severe pitting after etching. Depth profile of impurities measured by Time-of-Flight Secondary Ion Mass Spectrometry showed higher oxygen and hydrogen concentration in the pitted regions compared to non-pitted ones. The average quench field was (48 ± 15) mT and (63 ± 13) mT for TC1N1 and OCC1N2, respectively.

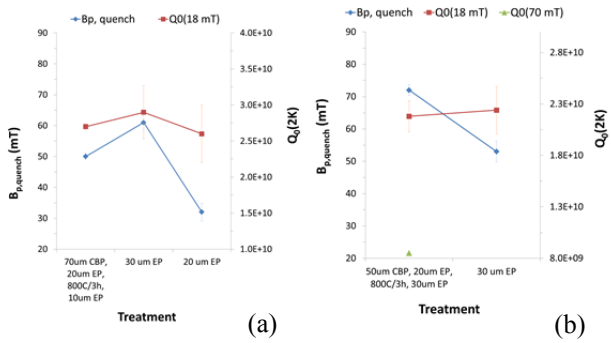

Figure 5: Evolution of the quench field and Q_0(2 K) at 18 mT and 70 mT for the 1.3 GHz cavity TC1N1 (a) and 1.5 GHz cavity OCC1N2 (b) after multiple material removal by EP, listed chronologically on the abscissa.

Table 6: Average R_{res}, Δ/k_BT_c and ℓ obtained from a fit of $R_s(T)$ with Eq. (1) and average R_{BCS}(4.3 K, 5 mT) EP on cavities TC1N1 and OCC1N2.

	TC1N1	OCC1N2
R_{BCS}(4.3 K) (nΩ)	495 ± 10	651 ± 13
R_{res} (nΩ)	2.6 ± 0.1	2.7 ± 0.1
Δ/k_BT_c	1.857 ± 0.001	1.83 ± 0.01
ℓ (nm)	26 ± 24	47 ± 9

DISCUSSION

Figure 6 shows a summary of the cavities' quench field as a function of the RRR of the ingot. EP often resulted in ~20% increase of the quench field, consistent with results on fine-grain cavities [11, 12].

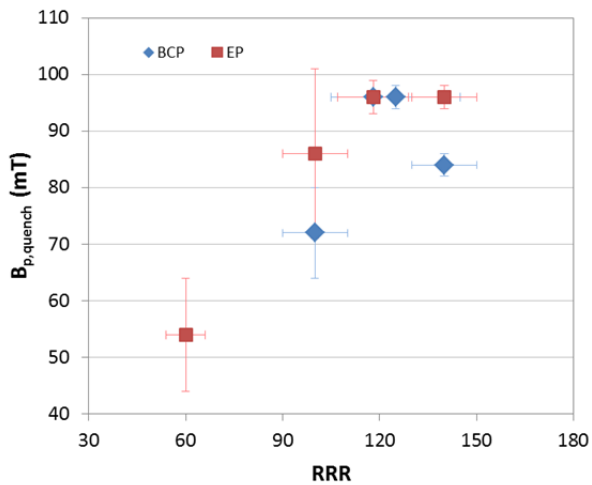

Figure 6: Average cavities' quench field as a function of the RRR of the ingot.

The low-field BCS surface resistance at 4.3 K is 500-650 nΩ at 1.3 GHz and 650-790 nΩ at 1.5 GHz, ~20% lower than that of RRR>300 Nb [13] because of the lower mean free path due to the higher concentration of interstitial impurities. An interesting result is that the residual resistance has no significant dependence on RRR in the range 60-150 and its value, ~2-3 nΩ, is comparable to the lowest values measured on fine-grain, RRR>300 cavities with similar treatments [11]. LTB reduces R_{BCS}, as a result of decreasing ℓ and increasing Δ/k_BT_c, and increases R_{res}, consistent with results from high-purity, fine-grain cavities [13]. HF rinse after LT restores R_{res} to the values prior to LTB, without changing R_{BCS}, resulting in higher Q_0-values at low field, consistent with results on high-purity, fine-grain cavities [14]. However, a stronger medium-field Q-slope after LTB makes the improvement of Q_0-values at 70 mT only marginal and such Q-slope is not altered significantly by HF rinse. Except for the cavity H3H4 in which the half-cells were annealed at 1200 °C prior to welding, an average Q_0-value of ~2×10^{10} at 2 K and 70 mT has been achieved with 1.3 GHz and 1.5 GHz medium-purity ingot Nb cavities, after BCP or EP only. This value is ~70% higher than the average Q_0-value measured at the same temperature and field on 7-cell, 1.5 GHz cavities for the upgrade of CEBAF, made of fine-grain, high-purity Nb with EP+LTB as final treatment. Doping medium-purity ingot Nb cavities either by nitrogen at 800 °C or by Ti above 1200 °C resulted in the even higher Q_0-values but the quench field often dropped below 70 mT.

The quench field of low-purity ingot Nb cavities was impacted by severe pitting after BCP, noting that pitting was observed on the discs prior to deep-drawing. The discs had been saw-cut from the ingot, then the thickness was adjusted on a lathe and a smooth finished was obtained by mechanical polishing with sand paper. Similar diffuse pitting was also noticed on discs cut by wire-electrodischarge machining (EDM) from a low-purity ingot from CBMM. Saw-cutting and machining on a lathe, as well as wire-EDM, had been used to slice discs from high-purity ingots but severe pitting did not occur after BCP, suggesting that too high interstitials could promote pitting. For comparison, a 1.5 GHz 5-cell cavity, a 650 MHz single-cell and a 400 MHz single-cell cavity were recently built from low-purity fine-grain Nb at Jefferson Lab and the quench fields at 2 K were 73 mT [15], 100 mT [16] and 26 mT [17], respectively.

CONCLUSIONS

The results from this study showed that:

- An average quench field of ~100 mT has been obtained in medium-purity (RRR~120-150) ingot Nb cavities at 2 K
- An average Q_0-value of ~2×10^{10} at 2 K and 70 mT has been obtained in medium-purity, 1.3-1.5 GHz ingot Nb cavities.
- An average low (2-3 nΩ) R_{res}-value was obtained, independent of RRR.
- Changes in low-field R_{BCS} and R_{res} by LTB and HF rinse are consistent with those obtained on high-purity, fine-grain Nb.
- Low-purity ingot Nb show diffuse pitting after BCP and higher concentration of O and H were found in pitted areas. The average quench field of low-purity ingot Nb cavities was ~50 mT but the defects causing the quench are not foreign inclusions in the material but pits resulting from chemical etching.

In summary, this study shows that medium-purity ingot Nb is a good material to build SRF cavities operating at medium gradients with higher efficiency and potentially lower cost than standard high-purity, fine-grain cavities.

ACKNOWLEDGMENT

We would like to acknowledge W. Singer and X. Singer at DESY for eddy-current scanning of the low-purity Nb discs, E. Zhou at NCSU for ToF-SIMS measurements, D. Forehand, J. Follkie, A. Anderson, C. Johnson, T. Harris, P. Kushnick at JLab for help with the cavity annealing, HPR, EP and cryogenic operations.

REFERENCES

[1] P. Kneisel et al., Nucl. Instrum. Methods A **774**, 133 (2015).
[2] W. Singer et al., Phys. Rev. ST Accel. Beams **16**, 012003 (2013).
[3] H. Padamsee, J. Knobloch, T. Hays, *RF Superconductivity for Accelerators*, (New York:Wiley, 1998), 217.
[4] W. Singer et al., Physica C **386**, 379 (2003).
[5] G. Ciovati et al., Mat. Sci. Eng. A **642**, 117 (2015).
[6] B. Aune et al., Phys. Rev. ST Accel. Beams **3**, 092001 (2000).
[7] P. Kneisel et al., IEEE Trans. Nucl. Sci. **30**(4), 3348 (1983).
[8] P. Dhakal et al., Phys. Rev. ST Accel. Beams **16**, 042001 (2013).
[9] A. Grassellino et al., Supercond. Sci. Technol. **26**, 102001 (2013).
[10] J. Halbritter, FZK 3/70-6, 1970.
[11] E. Kako et al., "Improvement of Cavity Performance in the Saclay/Cornell/DESY's SC Cavities", SRF'99, Albuquerque, November 1999, p. 179 (1999); http://www.JACoW.org
[12] J. Hao et al., "Low Temperature Heat Treatment Effect on High-Field EP Cavities", SRF'11, Travemünde, September 2011, p. 66 (2011); http://www.JACoW.org
[13] G. Ciovati, J. Appl. Phys. **96**, 1591 (2004).
[14] A. Romanenko et al., Phys. Rev. ST Accel. Beams **16**, 012001 (2013).
[15] P. Kneisel, JLab TN 13-047, 2013.
[16] P. Kneisel, JLab TN 14-018, 2014.
[17] F. He, Ph.D. Dissertation, Peking University, 2013.

ISBN 978-3-95450-178-6